Computers and Concrete, *Vol. 13, No. 4 (2014) 569-585*
DOI: http://dx.doi.org/10.12989/cac.2014.13.4.569

Three-dimensional finite element modeling of a transverse top-down crack in asphalt concrete

Majid R. Ayatollahi*, Sadjad Pirmohammad[a] and Karo Sedighiani[b]

Fatigue and Fracture Laboratory, Center of Excellence in Experimental Solid Mechanics and Dynamics, School of Mechanical Engineering, Iran University of Science and Technology, Narmak, Tehran, 16846, Iran

(*Received December 23, 2012, Revised February 22, 2014, Accepted February 25, 2014*)

Abstract. In this paper, a four-layer road structure consisting of an edge transverse crack is simulated using three-dimensional finite element method in order to capture the influence of a single-axle wheel load on the crack propagation through the asphalt concrete layer. Different positions of the vehicular load relative to the cracked area are considered in the analyses. Linear elastic fracture mechanics (LEFM) is used for investigating the effect of the traffic load on the behavior of a crack propagating within the asphalt concrete. The results obtained show that the crack front experiences all three modes of deformation i.e., mode I, mode II and mode III, and the corresponding stress intensity factors are highly affected by the crack geometry and the vehicle position. The results also show that for many loading situations, the contribution of shear deformation (due to mode II and mode III loading) is considerable.

Keywords: edge transverse crack; 3D finite element modeling; stress intensity factor; asphalt concrete; traffic load

1. Introduction

Asphalt concrete overlays are subjected to complex environmental and traffic loading conditions causing different types of deterioration in asphalt concrete pavements (Yoder and Witczak 1976). Asphalt concrete cracking is one of these damage mechanisms which decreases the service life of the asphalt concrete pavements and imposes significant costs to the road agencies. Good understanding of the cracking mechanism can be a reasonable way to reduce the costs of the maintenance processes. Majidzadeh *et al*. (1970) were among the first researchers who made use of fracture mechanics in order to study the fracture behavior of the cracked asphalt concrete pavements. Since then, the fracture mechanics approach has been frequently used by many other researchers (see for example Dongre *et al*. 1989, Kim and Hussein 1997, Molenaar *et al*. 2003, Li and Marasteanu 2004, Kim *et al*. 2008) to explore the cracking mechanism in asphalt concrete pavements. The stress intensity factors are fundamental parameter in the linear elastic fracture

*Corresponding author, Professor, E-mail: m.ayat@iust.ac.ir
[a]Ph.D., E-mail: s_pirmohammad@iust.ac.ir
[b]MSc., Student, E-mail: karo.sedigh@gmail.com

http://www.techno-press.org/?journal=cac&subpage=8 ISSN: 1598-8198 (Print), 1598-818X (Online)

mechanics (LEFM) which describe the singular stresses at the crack front. These factors can be employed for investigating the crack propagation within the asphalt concrete layer particularly when the asphalt concrete overlay is put into operation in the cold climate conditions (see Refs. Molenaar and Molenaar 2000, Tao *et al*. 2006, Tekalur *et al*. 2008). There are several papers in literature dealing with experimental investigation of crack growth in asphalt concretes. For instance, Pirmohammad and Ayatollahi (2014) and Im *et al*. (2014) have recently performed mixed mode fracture tests on asphalt mixtures using semi-circular test specimens. They have employed LEFM approach to analyze their test results.

According to a recent investigation performed by Al-Qadi and Wang (2009), pavement cracks sometimes nucleate and develop in the transverse direction relative to the wheel path. These transverse cracks can initiate on the surface of the asphalt concrete pavements and then propagate downward (top-down cracking) and also towards the road center. Top-down cracking can take place due to traffic loading, pavement aging and thermal stresses (as a result of extreme cooling rates), etc (Al-Qadi and Wang 2009, Emery 2007). Once a transverse crack nucleates on the pavement surface, the loads transferred from the traveling vehicles accelerate the crack propagation.

A review of literature indicates that many two-dimensional (2D) finite element analyses have been performed to study the mechanical behavior of cracked asphalt concrete overlays. For example, Zhou *et al*. (2008) and Kim *et al*. (2010) have calculated the stress intensity factors in a road structure containing a reflective crack using two-dimensional modeling. However, 2D finite element modeling is not able to consider some important aspects of crack growth such as out-of-plane mode of deformation (represented by K_{III}). Recent progresses in the field of asphalt concrete overlays illustrate the importance of three-dimensional (3D) modeling for cracked asphalt concrete pavements. Despite its complexity, 3D finite element modeling is more accurate and more reliable. 3D finite element techniques have been employed by several researchers in the past for analyzing the crack behavior in general 3D problems (see for example Pook 2000, 2013, Kotousov *et al*. 2010, Harding *et al*. 2010, Berto *et al*. 2012). These studies revealed a coupling between the shear modes of deformation (mode II and mode II) in 3D models of crack. Among very few 3D finite element investigations for asphaltic materials, Hadi and Bodhinayake (2003) studied the effect of moving wheel on the road structure but in the absence of any crack. In another research study, Garzon *et al*. (2010) simulated an airport road structure containing a reflective crack to investigate the effect of wheel load on the initiation and propagation of crack. Su *et al*. (2008) investigated the influence of some parameters like tire pressure on the shear stresses imposed to the asphalt concrete layer. Most recently, Ameri *et al*. (2011) studied the effects of traffic load on the stress intensity factors of a top-down crack located in the middle of the asphalt concrete overlay using 3D finite element simulations. However, they only calculated the stress intensity factors at the bottom part of crack front where the crack propagated downward. Meanwhile, the field studies conducted by Buttlar *et al*. (2004) show that the propagation of a transverse crack due to traffic loading is predominantly in the transverse direction rather than in the downward direction. Therefore, it is important to determine the stress intensity factors along the head of crack front where the crack propagates in the transverse direction.

In this paper, a large number of 3D finite element analyses are conducted on a typical road structure in order to investigate the effects of traffic load on the local deformation of a transverse crack embedded in the top asphalt concrete layer. An edge top-down crack is assumed within the asphalt concrete layer. The traffic loads induced from the vehicle wheels are applied on the cracked road at different positions of the vehicle wheels; and the stress intensity factors, K_I, K_{II}, and K_{III} are obtained along the head of the crack front.

2. Crack configuration in the road structure

A four-layer road structure consisting of hot mix asphalt (HMA) as top course, base, sub-base, and sub-grade course is used for determining the stress intensity factors along the crack front. An edge top-down crack of length c = 130 cm and depth b = 12 cm is assumed within the top layer of the pavement structure. The crack configuration and the positions of axle wheels are shown in Fig. 1. The geometry parameters assumed according to Fig. 1(b) can capture the main features of the investigated crack.

A vehicular loading with 80kN of single-axle is taken for the simulations, while each tire inserts 40kN to the asphalt concrete surface, as shown in Fig. 1(a). This amount of load is a typical value transferred from trucks on the road surface. The magnitude of each wheel pressure applied to the road surface with a rectangular area of 18 cm × 26 cm is 855kPa. The distance between the right and the left wheels is assumed to be 200cm which again is a typical value in trucks. The positions of the wheels are described by defining a coordinate system, where D states the right wheel distance from the edge of road, and L is the distance between the wheels axle and the crack plane (see Fig. 1(a). The crack is assumed to have been initiated from the road edge within the top layer (i.e. in the asphalt concrete layer of Fig. 1(a) and now is extending towards the centerline of the road. Thus, the crack head of quarter-circular shape (shown in detail in Fig. 1(b) is the focal zone for which the crack parameters should be calculated. The radius r of the quarter-circular arc is taken to be 12cm. The position of a point on the head of crack is defined by angle φ which takes the values of 0° and 90° at the road surface and the deepest point, respectively. The length and the width of the investigated block of road structure, T and W, are considered to be 900 cm and 600 cm, respectively. The ultimate goal of this research is to consider the effect of tire positions with respect to the crack plane on the stress intensity factors. The tire positions can be controlled by changing the values of distances D and L.

Crack propagation can occur under different modes of deformation including mode I, mode II, mode III or combinations of them. Mode I (known also as opening mode) occurs when crack faces

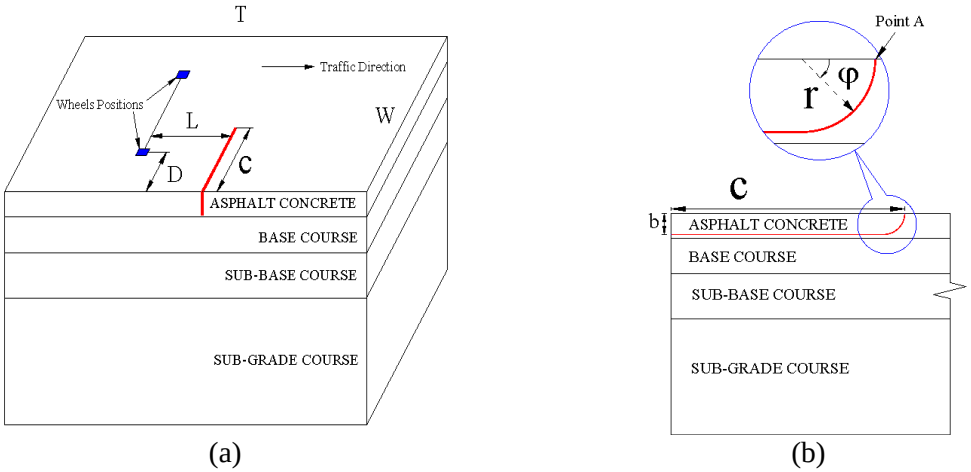

(a) (b)

Fig. 1 (a) Configuration of the cracked asphalt pavement, (b) side view and dimensions of a transverse crack

open without any sliding. Mode II (or sliding mode) takes place when the crack faces slide normal to the crack front without any opening, and mode III (or tearing mode) takes place when the crack faces slide parallel to the crack front without any opening. In the next section, a 3D finite element model is described by which the contributions of these modes are investigated in a cracked asphalt concrete layer.

3. Finite element modeling

The pavement layers including asphalt concrete, base layer, sub-base layer, and sub-grade layer are assumed to be homogenous and isotropic in the macro-scale with linear elastic behavior. These assumptions have been used frequently in the past by several researchers for investigating asphalt deformation (see for example Liang and Zhu 1995, Uddin *et al*. 1994, Novak *et al*. 2003). Moreover, traffic loading in the roads often occurs at a very short period; therefore, as a quasi-elastic material the HMA mixture properties can be represented by the Young's modulus and Poisson's ratio (see Ref. Zhou *et al*. 2008). Table 1 shows the mechanical properties of a road structure conventionally performed in Iran pavement systems together with the thickness of each layer (see Ref. Khavandy 2000). These data were used in the present finite element simulations. In order to apply the boundary conditions, the side faces of the model shown in Fig. 1(a) (i.e., front, rear, left and right faces) are fixed normal to the cut faces, while the other two degrees of freedom are free. The bottom face of the model (i.e., the bottom of the sub-grade layer) is also completely fixed in all directions.

Three-dimensional models of the road structure were analyzed using the second-order elements (20-node bricks) in the finite element code ABAQUS. The stress intensity factors K_I, K_{II} and K_{III}

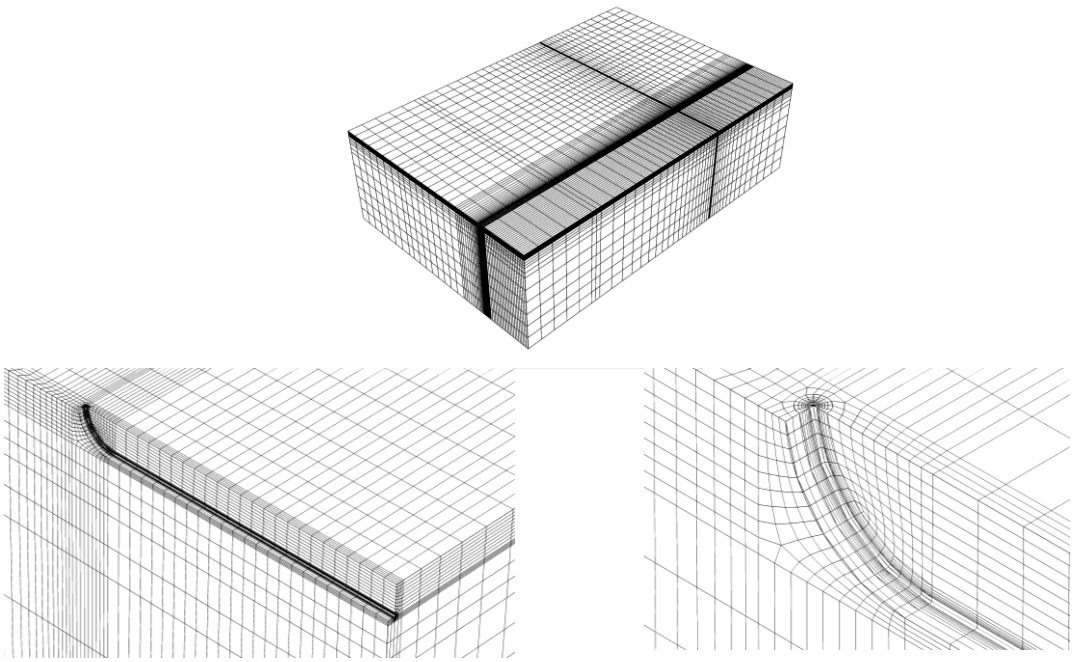

Fig. 2 Typical mesh pattern used for simulating the cracked road structure

Table 1 Mechanical properties and thickness of the road layers (see Khavandy 2000)

Layer	Young's modulus, E (MPa)	Poisson's ratio, υ	Thickness, t (cm)
Asphalt concrete	2760	0.35	14
Base	276	0.35	20
Sub-base	104	0.35	25
Sub-grade	34.5	0.45	200

for all finite element analyses were extracted directly from ABAQUS which employs an interaction integral method to compute the stress intensity factors for a crack under mixed-mode loading (see Refs. ABAQUS User's Manual 2007, Shih and Asaro 1988, Song and Paulino 2006, Yu *et al*. 2009). Fig. 2 shows the typical mesh pattern used for simulating the cracked road structure. The singular elements with nodes at quarter-point positions, which are highly recommended for crack modeling, were used for the first ring of elements around the crack front. In the circular region partitioned around the crack front where the contour integrals are calculated, the mesh was biased toward the crack front. The results of this work indicated that there is no significant variation in the contour integral values calculated for successive rings of the elements around the crack front. A mesh-convergence analysis was also performed to decide how many elements should be used for modeling.

4. Numerical results and discussion

A large number of 3D finite element analyses were successfully performed on the cracked road structure. The stress intensity factors K_I, K_{II} and K_{III} were determined for different points along the quarter-circular arc of the crack front (designated here as the head of crack) where the crack extension towards the middle of road is anticipated. Since finite element analyses are related to many different positions of the wheels with respect to the crack plane, for better understanding of the wheels positions with respect to the crack plane, it is reminded here that L designates the distance between the wheels axis and the crack plane. When L = 0, the case of D = 0.2 m represents the position where the wheels are symmetric relative to the point A along the crack front (see Fig. 1(b). By increasing D, this symmetry fades away; and for D = 1 m the right wheel is on top of the point A. The stress intensity factors calculated along the head of crack in terms of different wheel positions (L and D) are presented and discussed in the forthcoming sections.

4.1 Mode I stress intensity factor

Figs. 3(a) to 3(e) show the variations of the mode I stress intensity factor K_I along the head of crack versus the angle φ for different values of L and D. According to Fig. 3(a), when the transverse location of the wheels is fixed at D = 0.2 m, by moving the wheels towards the existing top-down crack in the range of L > 1.5 m, the mode I stress intensity factor increases significantly. For far distances i.e. when L > 3.5 m, K_I is almost zero. Therefore, when the crack is located far enough from the wheels, its deformation is negligible. Fig. 3(a) also shows that K_I has a maximum value at a certain value of φ for all longitudinal distances of the wheels from the crack (i.e., for all values of L). K_I first increases until reaching the maximum value, and then decreases. Meanwhile, as wheels approach the crack plane, the slope of K_I variations versus φ intensifies. For all values of

L, the maximum K_I occurs at about $\varphi = 5.6^{\circ}$.

The numerical results obtained for K_I have not been shown for L < 1.5 m. This is because when the wheels are near the crack plane, a top-down crack tends to close due to asphalt concrete layer downward deformation. A similar finding has also been reported earlier in Ameri *et al*. (2011). For such conditions, negative values are obtained for K_I from the finite element results. However, K_I is often assumed to be zero for a closed crack, since its effect on crack extension is negligible.

Another important result extracted from Fig. 3(a) is that, the mode I stress intensity factor (K_I) generally decreases for higher values of φ. This implies that the critical condition along the crack front takes place near the road surface, and consequently the crack tendency to extend transversely towards the middle of the road is higher than propagating vertically towards the underneath layers.

Figs. 3(b) to 3(e) show the results of K_I for D = 0.5 m, 0.7 m, 0.9m and 1m, respectively. The trends of K_I variations versus φ for all these values of D are similar to that for D = 0.2 m. Meanwhile, it is seen for each fixed value of L that there is a drop in the value of K_I as the distance D increases.

The results presented above indicates that opening deformation along the head of crack is observed for a wide range of L and D, and is considered as a major threat for the crack propagation and the deterioration of asphalt concrete pavement. Deterioration due to cracking is in particular of great importance for cold climates in which asphalt concretes are less deformable and hence brittle fracture and overall failure of the asphalt concrete becomes more probable. The research studies performed in the recent decades have been often focused on the understanding the mechanism of crack growth in mode I deformation, and many efforts have been made to select asphalt concretes with improved fracture resistance, in order to reduce their damage due to mode I crack growth (see for example Jung and Vinson 1993, Zubeck *et al*. 1996). Indeed, HMA mixture is a composite material made up of aggregate, air void, binder, and modifier. These components remarkably affect the fracture behavior of the HMA mixtures. Therefore, by selecting appropriate combinations of these components (see Refs. Li and Marasteanu 2010, Ayatollahi and Pirmohammad 2011) and also by applying a modified binder (particularly suitable for cold regions), the resistance of the asphalt concrete against cracking can be improved (see Refs. Kim *et al*. 2003, Casey *et al*. 2008).

4.2 Mode II stress intensity factor

The results obtained from 3D analyses showed that in addition to opening mode (mode I), the in-plane shear mode of deformation (mode II) occurs as well. Fig.4 presents the variations of mode II stress intensity factor K_{II} against φ for different positions of the wheels on the road with respect to the plane of transverse crack. It is useful to remind that the relative deformation of crack faces is for the cases that the signs of stress intensity factors are positive and the directions for the negative signs are opposite. For shear modes of deformation, both positive and negative signs of K_{II} and K_{III} contribute in the crack propagation, and the only difference is that the relative directions of the crack face deformation reverse by switching the sign of K_{II} or K_{III}. However, for mode I deformation the positive sign implies that the crack faces open and contribute in the crack extension, while the negative sign denotes that crack faces close with almost no effect on crack extension. Therefore, the results which are shown in sections 4-2 and 4-3 for mode II and mode III stress intensity factors will be presented for both positive and negative signs of K_{II} and K_{III} with more emphasis on their absolute values rather than their signs.

The numerical results obtained for K_{II} are first discussed in more details for the case of D = 0.2

m (Fig. 4(a)) and then are elaborated for other transverse distances D. As shown in Fig. 4(a), when the wheels approach the crack plane (i.e., L decreases), the magnitude of K_{II} initially increases.

However, for small distances between the wheels and the crack plane (e.g. L = 0.25 m), there is again a reduction in the value of K_{II}. Similar to the results shown for the opening mode, when

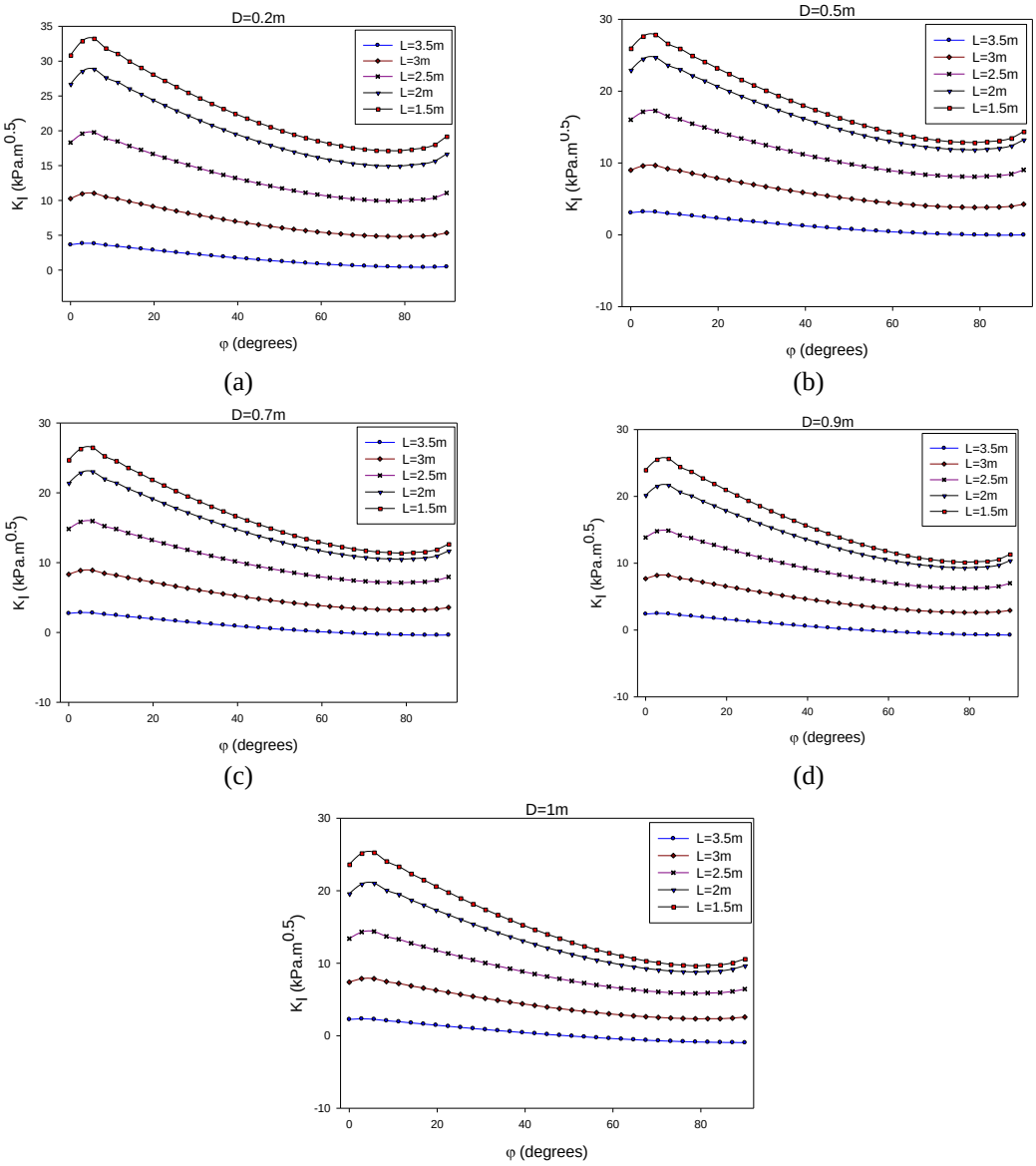

Fig. 3 Mode I stress intensity factor for different values of φ, L and a) D = 0.2 m, b) D = 0.5 m, c) D = 0.7m, d) D = 0.9 m, e) D = 1 m

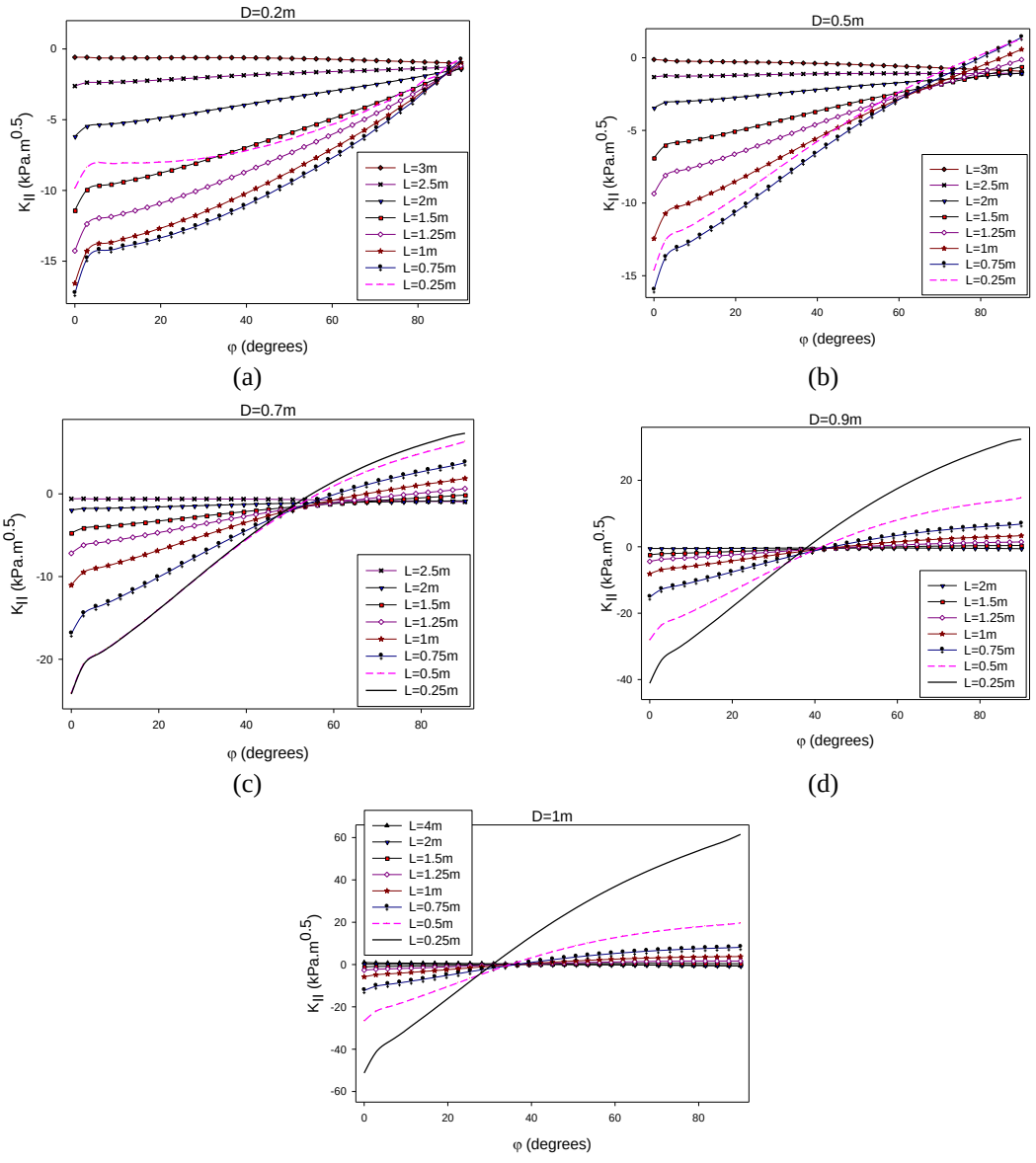

Fig. 4 Mode II stress intensity factor for different values of φ, L and a) D = 0.2 m, b) D = 0.5 m, c) D = 0.7 m, d) D = 0.9 m, e) D = 1m

wheels are far enough from the crack (for the cases that L > 3 m), the influence of traffic load on mode II deformation is negligible. On the other hand, for all the wheel distances L from the crack, by increasing φ, first the magnitude of K_{II} decreases sharply and then decreases gradually to reach nearly zero values at $\varphi = 90^{\circ}$. Similar to the results obtained for K_I, the magnitudes of K_{II} in regions

near the road surface (lower values of φ) are significantly more than those in the deepest part of

the crack front where φ tends towards 90°. The combined effects of mode I and mode II stress intensity factors make the transverse crack more susceptible to extension at lower values of φ (near the road surface) than higher values of φ. Therefore, the variations of K_{II} also suggest that the crack tends to grow towards the middle of the asphalt concrete layer in the transverse direction rather than to develop downwards. It is worth noting that Buttlar *et al*. (2004) also observed through field investigations that a crack within the asphalt concrete layer often extends in the transverse direction, which is consistent with theoretical results obtained in the present research.

Fig. 4(b) shows the results of K_{II} for the transverse distance of D = 0.5 m. The general trend for variations of K_{II} are similar to the results of D = 0.2 m, with this important difference that K_{II} reduces to zero at angles φ around 75° and then begins to increase while its sign changes from negative to positive. Therefore, the direction for relative sliding of crack faces is not the same for the entire values of φ, and it changes at a specific value of φ depending on the longitudinal distance L. By comparing Figs. 4(a) to 4(e), it is found that by increasing D, the magnitude of φ at which the sign of K_{II} changes decreases. The maximum in-plane shear deformation ($K_{II} \approx 50 kPa.m^{0.5}$) takes place when the axle is located in the position of D = 1 m and L = 0.25 m i.e. when one of the wheels is just before the crack plane and in front of the head of crack. As shown earlier in Fig. 3, the maximum value of K_I was about $35 kPa.m^{0.5}$. Therefore, in some particular wheel positions K_{II} is significantly higher than K_I.

Most of the research studies reported in the past decades on the fracture behavior of the asphalt concretes focused on the mode I fracture mechanism. The researchers (for example Kim and Hussein 1997, Molenaar *et al*. 2003, Molenaar and Molenaar 2000, Wagoner *et al*. 2005) have used several test specimens such as single edge notched beam (SENB), disk-shaped compact tension (DC-T), semi-circular bend (SCB), etc. to evaluate and improve the fracture resistance of asphalt concretes under mode I loading. Very few investigations have been reported concerning mixed mode I/II fracture behavior of asphalt concretes. While, no standard test method has been proposed for measuring the mode II fracture resistance of asphalt concretes (see Zhou *et al*. 2008), it is sometimes assumed that mode I and mode II have the same fracture properties (see for example Lytton 1989). As our results showed, there are some cases in asphalt concretes that the effect of mode II deformation on transverse cracks is higher than that of mode I deformation. Hence, more investigations are required to better understand the crack growth mechanisms in HMA mixtures under mode II and mixed mode I/II loading conditions.

4.3 Mode III stress intensity factor

By approaching the vehicle axle towards the crack plane, in addition to K_I and K_{II}, out-of-plane shear mode (K_{III}) was also observed in crack deformation. Fig. 5(a) shows the variations of K_{III} against φ for D = 0.2 m and different values of L. Similar to the results shown in Fig. 3(a) and Fig. 4(a) for K_I and K_{II}, the mode III stress intensity factor K_{III} was also negligible for the cases that wheels were far enough from the crack (i.e., when L > 3 m). By approaching the wheels towards the crack, K_{III} increases for all values of φ (except for the case of L = 0.25 m which shows different results). As a general trend, the magnitude of K_{III} first decreases by φ and then increases. It is clear from Fig. 5(a) that when D = 0.2 m the maximum value of K_{III} occurs at φ = 90°. Fig. 5(b) shows the results of K_{III} for D = 0.5 m. Similar to the results for D = 0.2 m, the magnitude of K_{III} first decreases and then increases gently, but the maximum value of K_{III} takes place on the road surface (i.e., at φ = 0°). The general trends of K_{III} variations against φ for D = 0.7 m, 0.9 m, and 1 m are different from those of D = 0.2 m and 0.5 m. However, the maximum magnitudes of K_{III} are

still observed at $\varphi = 0°$. In some cases, there is a switch in the sign of K_{III} along the head of crack. By moving the wheels away from the crack plane (i.e. for larger distances D), the value of φ at which the sign of K_{III} reverses, decreases.

Fig. 6 presents the influence of parameters D and L on the stress intensity factors K_I, K_{II} and K_{III}. The numerical results have been plotted for $\varphi = 5.6^{\circ}$ since the results obtained from the finite element analysis for $\varphi = 0^{\circ}$ may contain some numerical errors. This is because LEFM is based upon the assumption of the continuity of the crack front. This assumption is no longer valid at

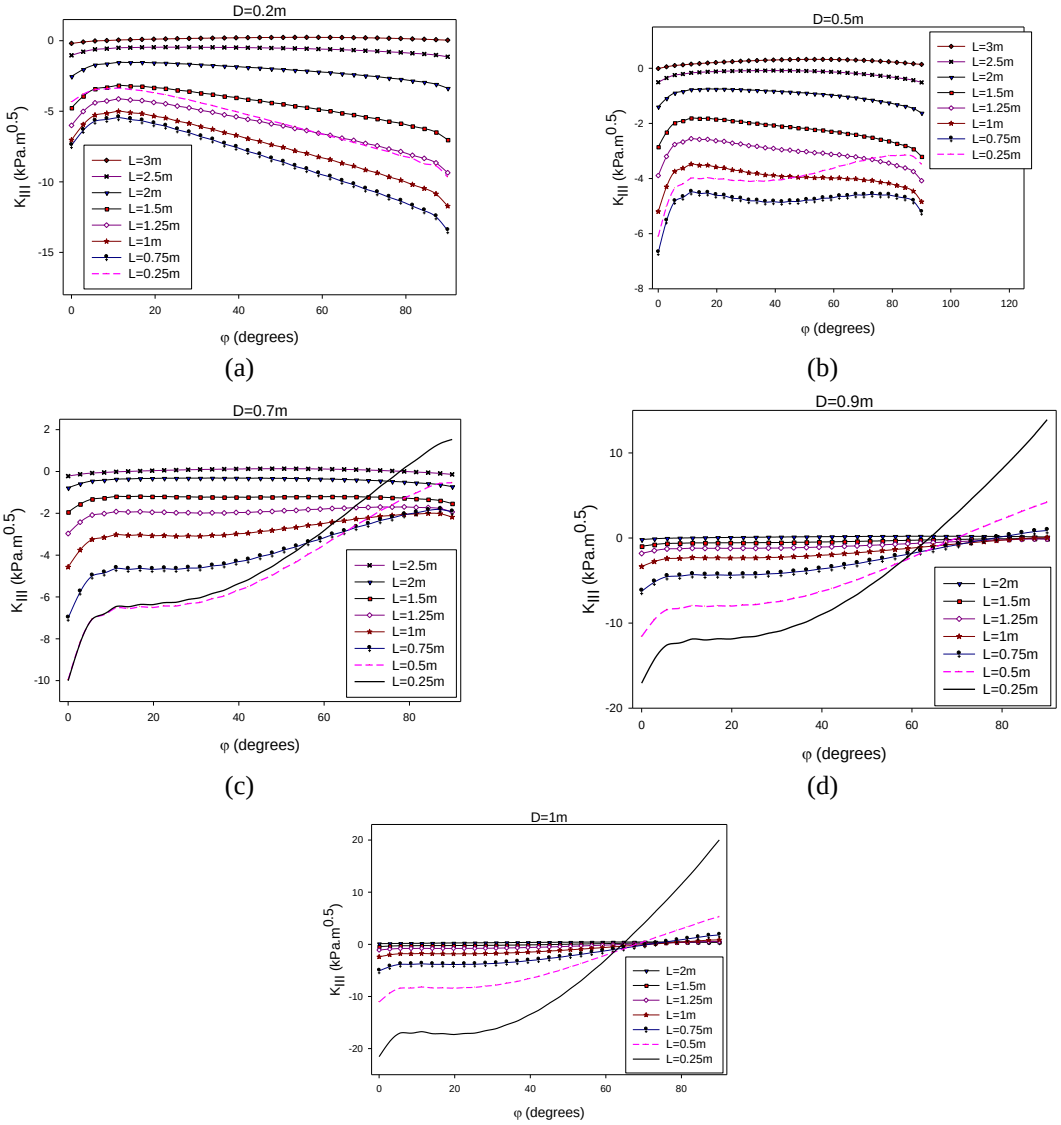

Fig. 5 Mode III stress intensity factor for different values of φ, L and a) D = 0.2 m, b) D = 0.5 m, c) D = 0.7 m, d) D = 0.9 m, e) D = 1 m

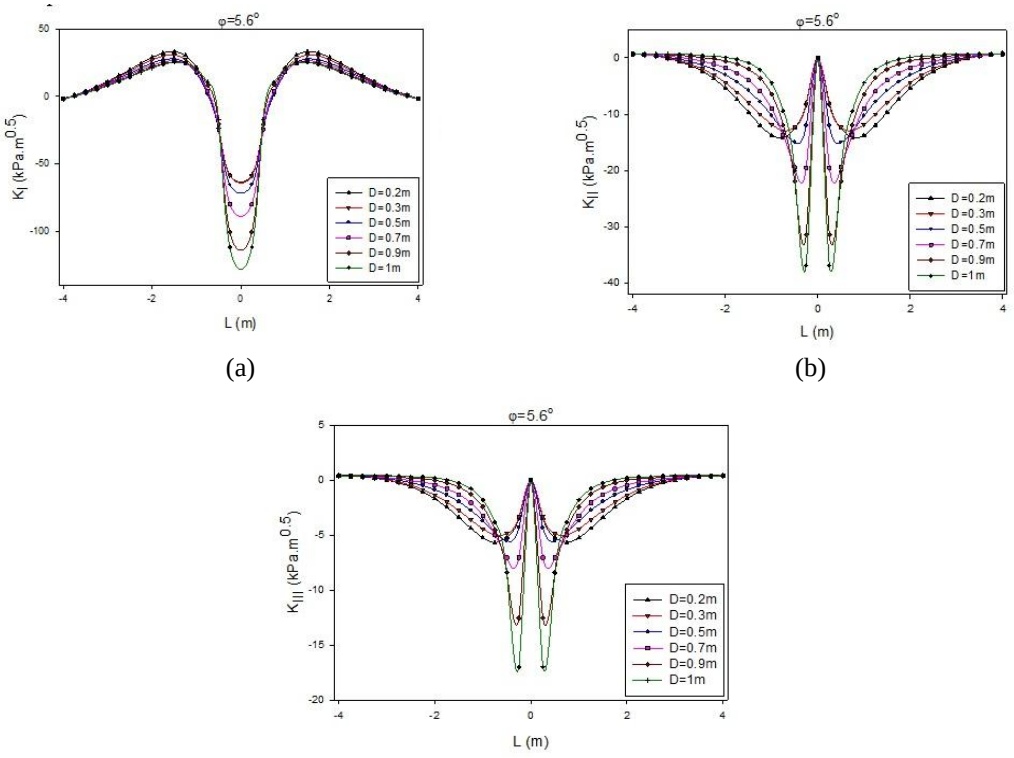

Fig. 6 Variations of crack front parameters, a) K_I, b) K_{II}, c) K_{III}, versus L for $\varphi = 5.6°$ and different values of D

corner points where the crack front intersects the free surface of the body. This accuracy loss is caused by a combination of the relative coarseness of the mesh, especially in this end region where the crack depth varies rapidly, as well as from theoretical points related to the appropriateness of line spring modeling at the end regions of the crack front. It has been shown that the order of the stress singularity at the end points depends on the material property and the intersection angle (see Refs. Pook 1993, Pook 1995). Pook (1993) showed that the values of crack front parameters predicted by numerical methods at the corner points are not reliable, and the use of quarter-point finite elements that model the square-root singularity of stresses and strains does not produce accurate results near such points. More details on this subject can be found in Parks (1981) and Parks *et al*. (1981).

According to Fig. 6(a), when the wheels approach the crack plane (or L decreases), the magnitude of K_I first increases against L (or the crack faces open) and then starts decreasing until the crack faces close completely. In the region $|L|<0.5$ m, the sign of K_I is negative indicating that mode I deformation has negligible effect on the process of crack extension. A similar trend is observed in Fig. 6(b) for K_{II} variations against L i.e., the magnitude of K_{II} first increases and then sharply decreases to reach zero for all values of D. The trends for the influence of parameters D and L on K_{III} was very similar to those of K_{II} with this difference that the magnitude of K_{III} was lower compared with the magnitude of K_{II}. When the wheels are located exactly on the crack line (L = 0), the loading conditions would be symmetric relative to the crack plane. Therefore, in such a

condition, no relative sliding or tearing movement takes place between the crack faces and, as expected, $K_{II} = K_{III} = 0$ (see Fig. 6). Moreover, the results obtained from the finite element analyses are identical when the wheel axle is in the distances of same magnitudes (i.e., + L and –L) from the crack plane.

4.4 Proportion of shear deformation to total deformation

The results obtained from finite element analyses showed that different locations of vehicle on the road cause different types of deformation including tensile (opening) mode and shear (sliding or tearing) modes in the vicinity of the crack front. As mentioned earlier, opening mode (mode I) has been widely investigated for asphalt mixtures by several researchers, while shear modes especially mode III has received very little attention. Here, the proportion of shear deformation relative to total deformation is approximated by using the concept of energy release rate G which is defined for different modes of loading as

$$G_I = \frac{K_I^2}{E},\ G_{II} = \frac{K_{II}^2}{E},\ G_{III} = \frac{K_{III}^2}{2\mu},\ G = G_I + G_{II} + G_{III} \tag{1}$$

where, E and μ are the Young's modulus and the shear modulus, respectively. The contribution of shear deformation can be written as $\frac{G_{II}+G_{III}}{G}$. More details about the parameter G and reviews of its associated fracture criteria can be found in Berto and Lazzarin (2009, 2013).

Fig.7 shows the variations of $\frac{G_{II}+G_{III}}{G}$ against φ for different positions of the wheels. It is observed from Fig. 7(a) for D = 0.2 m that when the wheels are far from the crack plane (large L values), shear modes have negligible contribution in the total deformation near the crack front. By approaching the wheels towards the crack plane, the shear modes become dominant relative to the tensile mode and when the wheels are very close to the crack, the total deformation is almost due only to shear modes. As shown in Figs.7a to 7c, similar trends are observed for the cases of D = 0.5 m and D = 0.7 m.

It is finally noted that almost all of the finite element analyses performed by researchers in the past to study the mechanical behavior of cracked asphalt concrete pavements deal with two-dimensional models and concentrate mainly on bottom-up or reflective cracks. Two-dimensional models are able to calculate only the mode I and mode II stress intensity factors. The three-dimensional crack models investigated recently by Ameri *et al*. (2011) have given the results only at a fixed point along the crack front and are suitable for downward crack growth. The numerical results displayed in the present research showed that shear modes play an important role in crack deformation for top-down cracks under traffic loading. In particular, the mode III stress intensity factor K_{III} is strongly present along the head of a transverse crack and can influence the process of crack growth in the transverse direction significantly.

It is worth mentioning that asphalt concrete is a temperature dependant material, and its mechanical properties such as elasticity modulus vary with daily ambient temperature fluctuations. It is well-known that the elasticity modulus of asphaltic materials increases as the ambient temperature decreases. The fracture toughness of asphalt concretes is also temperature dependent (see e.g. Miao *et al*. 2010) such that cracks within asphalt concretes would be more prone to propagate at cold climate regions (more details can be found in Pirmohammad and Ayatollahi 2014).

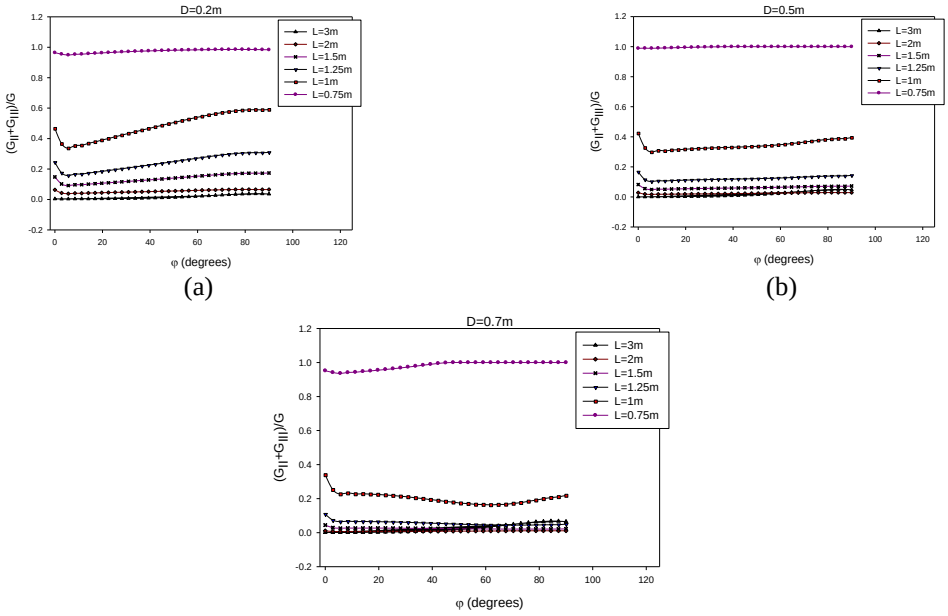

Fig. 7 Variations of $(G_{II}+G_{III})/G$ versus φ for different values of L and for a) D = 0.2 m, b) D = 0.5 m, c) D = 0.7 m

4.5 Assessment based on a fracture criterion

One might be interested to study if a pre-existing crack within an asphalt concrete layer grows under the vehicle loads. For this purpose, it is essential to compare the numerically determined stress intensity factors (K_I, K_{II} and K_{III}) at the crack front with an appropriate fracture criterion. Numerous 2D and 3D mixed-mode fracture criteria have been developed in the past by researchers, some of which are listed below:

For 2D fracture criteria:

- *Maximum tangential stress* (e.g. Erdogan and Sih 1963, Ayatollahi and Torabi 2010).
- *Generalized maximum tangential stress (e.g. Smith et al. 2001, Ayatollahi et al. 2006).*
- *Maximum energy release rate (e.g. Hussain et al. 1974).*
- *Strain energy density (e.g. Sih 1974, Lazzarin and Berto 2005).*

For 3D fracture criteria:

- *Criterion by Sih (Sih 1974, 1990).*
- *Criterion by Schöllmann et al. (Schöllmann et al.2001, 2002).*
- *Criterion by Pook* (Pook 1985, 2000).

Since the present paper deals with three-dimensional modeling of road structures hence, from the above fracture criteria, the criterion suggested by Pook (1985, 2000) was chosen to show how one can predict the onset of crack growth within the asphalt concrete layer.

Table 2 The values of K_I, K_{II} and K_{III} together with corresponding values of $K_{V,I,II,III}$ in three different positions of wheels

No.	wheels position	K_I $(kPa.m^{0.5})$	K_{II} $(kPa.m^{0.5})$	K_{III} $(kPa.m^{0.5})$	$K_{V,I,II,III}$ $(kPa.m^{0.5})$
1	L=1.5 m & D = 0.2 m (φ=5.6°)	33.3	9.7	3.4	50.6
2	L = 0.25 m & D = 1 m (φ=90°)	0	61.5	20.0	110.7
3	L = 0.25 m & D = 1 m (φ=5.6°)	0	-36.8	-17.0	72.4

According to Pook's criterion, a three-dimensional crack extends when the value of spatial comparative stress intensity factor $K_{V,I,II,III}$ given in Eq. (2) is equal or higher than the asphalt concrete fracture toughness K_{Ic}. $K_{V,I,II,III}$ is calculated from (Pook 2000)

$$K_{V,I,II,III} = \frac{K_{V,I,II}(1+2\upsilon) + \sqrt{K_{V,I,II}^2(1-2\upsilon)^2 + 4K_{III}^2}}{1.5} \tag{2}$$

where, υ is the Poisson's ratio, and the plane comparative stress intensity factor $K_{V,I,II}$ is calculated from

$$K_{V,I,II} = \frac{0.83K_I + \sqrt{0.4489K_I^2 + 3K_{II}^2}}{1.5} \tag{3}$$

Table 2 shows K_I, K_{II} and K_{III} together with corresponding calculated values of in three different positions of wheels. These wheel positions were selected in a way to have $K_{V,I,II,III}$ maximum values for K_I (No. 1 in Table 2), for K_{II} (No. 2 in Table 2) and for K_{III} (No. 3 in Table 2). Tekalur *et al*. (2008) have reported the value of K_{Ic} = 110kPa.m$^{0.5}$ for asphalt concretes. For example according to Table 2, in the wheels position of L = 0.25 m & D = 1 m and at φ = 90° (No. 2 in Table 2), $K_{V,I,II,III}$ is larger than the asphalt concrete fracture toughness K_{Ic} = 110kPa.m$^{0.5}$. Therefore, the fracture criterion suggested by Pook (1985, 2000) predicts that the crack within the asphalt concrete layer would develop for this position of the wheels. Similar analyses can be performed for other positions of the wheels to find more critical positions for crack growth in asphalt layers.

5. Conclusions

- A 3D model of a typical road structure containing a transverse top-down crack on the road surface was simulated using the finite element method.
- A large number of finite element analyses were performed to study the effect of vehicle location on the stress intensity factors along the crack front. The numerical results showed that the head of crack front generally experiences all three modes of deformation namely mode I, mode II, and mode III.
- The stress intensity factors K_I, K_{II}, and K_{III} vary at different points along the head of crack and are highly affected by the wheels locations with respect to the crack plane (L and D).
- For all longitudinal distances of the axle from the crack plane (L), the maximum values of K_I and K_{II} occur at the points near the road surface along the head of crack indicating the crack tendency to grow in the transverse direction rather than extending downwards.

- A review of literature indicates that the shear modes deformation especially mode III have received very little attention, and their importance has been neglected by researchers. However, the results obtained in this research showed that for some locations of the wheels, the magnitude of K_{II} was significantly greater than that of K_I. In some cases, the mode III stress intensity factor K_{III} was the dominant crack parameter. Therefore, the shear modes of deformation along the crack front should not be ignored in the life estimation of road structures containing transverse cracks.

References

ABAQUS, User's Manual (2007), *Dassault Systemes Simulia Corp*, Providence, Rhode Island, V 6.7.

Al-Qadi, I. and Wang, H. (2009), *Evaluation of Pavement Damage Due to New Tire Designs*, Research Report ICT-09-048.

Ameri, M., Mansourian, A., Heidary-Khavas, M., Aliha, M.R.M. and Ayatollahi, M.R. (2011), "Cracked asphalt pavement under traffic loading – A 3D finite element analysis", *Eng Fract Mech*, **78**, 1817-1826.

Ayatollahi, M.R. and Aliha, M.R.M. (2006), "On determination of mode II fracture toughness using semicircular bend specimen", *Int. J. Solids Struct*., **43**, 5217-5227.

Ayatollahi, M.R. and Pirmohammad, S. (2011), "Effect of asphalt cement type on the fracture behavior of asphalt mixtures", *9th In fracture conference*, Istanbul, 313-319.

Ayatollahi, M.R. and Torabi, A.R. (2011), "Failure assessment of notched polycrystalline graphite under tensile-shear loading", *Mater. Sci. Eng., A.*, **528**, 5685-5695.

Berto, F. and Lazzarin, P. (2009), "A review of the volume-based strain energy density approach applied to V-notches and welded structures", *Theor Appl Fract Mech*, **52** (3), 183-194.

Berto, F. and Lazzarin, P. (2014), "Recent developments in brittle and quasi-brittle failure assessment of engineering materials by means of local approaches", *Mater. Sci. Eng. R.*, **75**, 1-48.

Berto, F., Lazzarin, P., Kotousov, A. and Pook, L.P. (2012), "Induced out-of-plane mode at the tip of blunt lateral notches and holes under in-plane shear loading", *Fatigue. Fract. Eng. Mater. Struct.*, **35**(6), 538-555.

Buttlar, W.G., Armando, D.C. and Garzon, J. (2004), *Development of New Methodologies for Mechanistic Design of Asphalt Overlays*, Research report, Department of civil and environmental engineering, University of Illinois, Urbana Champaign.

Casey, D., McNally, C., Gibney, A. and Gilchrist, M.D. (2008), "Development of a recycled polymer modified binder for use in stone mastic asphalt", *J. Resour. Conserv. Recycl*., **52**, 1167-1174.

Dongre, R., Sharma, M.C.l. and Anderson, D.A. (1989), "Development of fracture criterion for asphalt mixes at low temperatures", *Transp. Res. Rec*., **1228**, 94-105.

Erdogan, F. and Sih, G.C. (1963), "On the crack extension in plates under plane loading and transverse shear", *J Basic Eng*, **85**, 519-525.

Emery, J. (2007), "Mitigation of asphalt pavement Top-Down cracking", *4th Int SIIV Congress*, Palermo, Italy, 12-14.

Garzon, J., Duarte, C.A. and Buttlar, W.G. (2010), "Computational simulations of a full-scale reflective cracking test", *FAA Worldwide Airport Technology Transfer Conference*, Atlantic City, New Jersey, USA.

Hadi, M.N.S. and Bodhinayake, B.C. (2003), "Non-linear finite element analysis of flexible pavements", *J. Adv. Eng. Software*, **34**, 657-662.

Harding, S., Kotousov, A., Lazzarin , P. and Berto, F. (2010), "Transverse singular effects in V-shaped notches stressed in mode II", Int *J Fract*, **164** (1), 1-14.

Hussain, M.A., Pu, S.L. and Underwood, J. (1974), "Strain energy release rate for a crack under combined mode I and mode II", *Fracture analysis ASTM STP 560 American Society for Testing and Materials, Philadelphia*, 2-28.

Im S., Ban H., Kim Y.R. (2014), "Characterization of mode-I and mode-II fracture properties of fine aggregate matrix using a semicircular specimen geometry", *Constr Build Mater*, **52**, 413-421.

Jung, D. and Vinson, T.S. (1993), "Low temperature cracking resistance of asphalt concrete mixtures", *J. Assoc. Asphalt Paving Technol.*, **62**, 54-92.

Khavandy, A. (2000), Designing Flexible Pavements in Iran Using Mechanistic Methods, Dissertation for MSc. Degree, Iran University of Science and Technology.

Kim, H., Buttlar, W.G. and Chou, K.F. (2010), "Mesh-Independent fracture modeling for overlay pavement system under heavy aircraft gear loadings", *J. Transp. Eng.*, **136**, 370-378.

Kim, H., Wagoner, M.P. and Buttlar, W.G. (2008), "Numerical fracture analysis on the specimen size dependency of asphalt concrete using a cohesive softening model", *Constr. Build. Mater.*, **23**, 2112-2120.

Kim, K.W. and Hussein, M.E. (1997), "Variation of fracture toughness of asphalt concrete under low temperatures", *Constr. Build. Mater.*, **11**, 403-411.

Kim, K.W., Kweon, S.J., Doh, Y.S. and Park, T.S. (2003), "Fracture toughness of polymer modified asphalt concrete at low temperatures", *Canadian J Civ Eng*, **30**, 406-413.

Kotousov, A., Lazzarin, P., Berto, F. and Harding, S. (2010), "Effect of the thickness on elastic deformation and quasi-brittle fracture of plate components", *Eng Fract Mech*, **77** (11), 1665-1681.

Lazzarin, P. and Berto, F. (2005), "From Neuber's elementary volume to Kitagawa and Atzori's diagrams: an interpretation based on local energy", *Int J. Fract.*, **135**, 33-38.

Liang, R.Y. and Zhu, J.X. (1995), "Dynamic analysis of infinite beam or modified Vlasov subgrade", *J. Transp Eng*, 434–443.

Li, X. and Marasteanu, M.O. (2004), "Evaluation of the low temperature fracture resistance of asphalt mixtures using the semi-circular bend test", *J. Assoc. Asphalt Paving Technol.*, **73**, 401-426.

Li, X.J. and Marasteanu, M.O. (2010), "Using semi-circular bending test to evaluate low temperature fracture resistance for asphalt concrete", *J. Exp. Mech.*, **50**, 867-876.

Lytton, R.L. (1989), "Use of geotextiles for reinforcement and strain relief in asphaltic concrete", *Geotext Geomembr*, **8**, 217-237.

Majidzadeh, K., Kaufmann, E.M. and Ramsamooj, D.V. (1970), "Application of fracture mechanics in the analysis of pavement fatigue", *J. Assoc. Asphalt Paving Technol.*, **40**, 227-246.

Miao Y., He T.G, Yang G., Zheng J.J. (2010), "Multi-domain hybrid boundary node method for evaluating top-down crack in Asphalt pavements", *Eng Analysis Boundary Elements*, **34**, 755-760.

Molenaar, J.M.M., Liu, X. and Molenaar, A.A.A. (2003), "Resistance to crack-growth and fracture of asphalt mixture", *6th Int RILEM Symposium on Performance Testing and Evaluation of Bituminous Materials*, Zurich, Switzerland, 618-625.

Molenaar, J.M.M. and Molenaar, A.A.A. (2000), "Fracture toughness of asphalt in the semi-circular bend test", *2nd Eurasphalt and Eurobitume Congress*, Barcelona, Spain, 509-517.

Novak, M., Birgisson, B. and Roque, R. (2003), "Near-surface stress states in flexible pavements using measured radial tire contact stresses and ADINA", *J. Comput Struct*, **81**, 859–870.

Parks, D.M. (1981), "The Inelastic Line Spring: Estimates of Elastic-Plastic Fracture Mechanics Parameters for Surface-Cracked Plates and Shells", *J. Pressure Vessel Technol.*, **13**, 246–254.

Parks, D.M., Lockett, R.R. and Brockenbrough, J.R. (1981), "Stress intensity factors for surface-cracked plates and cylindrical shells using line spring finite elements", *Proc. of the Winter Annual Meeting, ASME*, Washington, DC.

Pirmohammad, S. and Ayatollahi M.R. (2014), "Fracture resistance of asphalt concrete under different loading modes and temperature conditions", *Constr Build Mater*, **53**, 235-242.

Pook, L.P. (1993), "A finite element analysis of the angle crack specimen, mixed mode fatigue and fracture", *Rossmanith, Miller, Mechanical Engineering Publications, editors. ESIS*, **14**, 285–302.

Pook, L.P. (1985), "Comments on fatigue crack growth under mixed modes I and III and pure mode III loading", *Multiaxial Fatigues*, In: Miller, K.J., Brown, M.W, 249-263.

(Eds.), ASTM STP853, American Society for Testing and Materials, Philadelphia.

Pook, L.P. (2000), "Finite element analysis of corner point displacements and stress intensity factors for narrow notches in square sheets and plates", *Fatigue Fract Eng Mater Struct*, **23**(12), 979-992.

Pook, L.P. (2000), "Linear elastic fracture mechanics for engineers: theory and application", *WIT press*, Southampton.
Pook, L.P. (2013), "A 50-year retrospective review of three-dimensional effects at cracks and sharp notches", *Fatigue Fract Eng Mater Struct*, **36** (8), 699-723.
Pook, L.P. (1995), "On fatigue crack paths", *J. Fatigue*, **17**, 5-13.
Shih, C.F. and Asaro, R.J. (1988), "Elastic-plastic analysis of cracks on bimaterial interfaces- part I-small scale yielding", *J. Appl. Mech*., **55**, 299-316.
Schöllmann, M., Kullmer, G., Fulland, M. and Richard, H.A, (2001),"A new criterion for 3D crack growth under mixed mode (I+II+III) loading", *Proceeding of 6th Int. Conference of Biaxial/Multiaxial Fatigue and Fracture*, **2**, 589-596.
Schöllmann, M., Richard, H.A., Kullmer, G. and Fulland, M. (2002), "A new criterion for the prediction of crack development in multiaxially loaded structures ", *Int J Frac*, **117**, 129-141.
Sih, G.C. (1974), "Strain-energy-density factor applied to mixed mode crack problems", *Int. J. Fract*., **10**, 305-321.
Sih, G.C. (1990), Mechanics of fracture initiation and propagation, Kluwer Academic publishers, Dodrecht, Netherlands.
Smith, D.J., Ayatollahi, M.R. and Pavier, M.J. (2001), "The role of T-stress in brittle fracture for linear elastic materials under mixed mode loading", *Fatigue Fract Eng Mater Struct*, **24**, 137-150.
Song, S.H. and Paulino, G.H. (2006), "Dynamic stress intensity factors for homogeneous and smoothly heterogeneous materials using the interaction integral method", *J. Solids Struct*., **43**, 4830-4866.
Su, K., Sun, L., Hachiya, Y. and Maekawa, R. (2008), "Analysis of shear stress in asphalt pavements under actual measured tire-pavement contact pressure", *6th ICPT*, Sapporo, Japan.
Tao, X., Yanjun, Q., Zezhong, J. and Changfa, A. (2006), "Study on compound type crack propagation behavior of asphalt concrete", *Key Eng Mater*, **324-325**, 759-762.
Tekalur, S.A., Shukla, A., Sadd, M. and Lee, K.W. (2008), "Mechanical characterization of a bituminous mix under quasi-static and high-strain rate loading", *Constr. Build. Mater*., **23**, 1795-1802.
Uddin, W., Zhang, D. and Fernandes, F. (1994), "Finite element simulation of pavement discontinuities and dynamic load response", *Transp. Res. Rec*., **1448**, 100-106.
Wagoner, M.P., Buttlar, W.G. and Paulino, G.H. (2005), "Disk-shaped compact tension test for asphalt concrete fracture", *J. Exp. Mech*., **45**, 270-277.
Yoder, E. and Witczak, M. (1976), *Principles of Pavement Design*, Second Ed., John Wiley and sons Inc., New York.
Yu, H., Wu, L., Guo, L., Du, S. and He, Q. (2009), "Investigation of mixed-mode stress intensity factors for non-homogeneous materials using an interaction integral method", *J. Solids Struct*., **46**, 3710-3724.
Zhou, F., Hu, S., Hu, X. and Scullion, T. (2008), *Mechanistic-empirical Asphalt Overlay Thickness Design and Analysis System*, Report No. FHWA/TX-09/0-5123-3, Texas Transportation Institute, College Station.
Zubeck, H.K., Zeng, H.Y., Vinson, T.S. and Janoo, V.C. (1996), "Field validation of thermal stress restrained specimen test", *Transp. Res. Rec*., **1545**, 67-74.

CC